

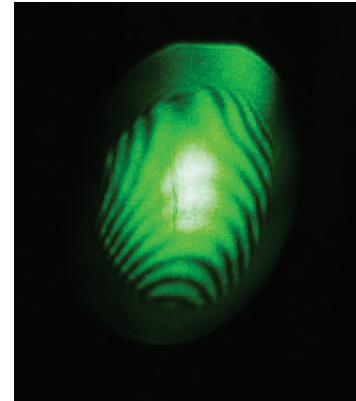
Low-frequency ground deformation observed by the geophysics interferometer (GIF) in the KAGRA tunnel

Akito Araya [1], Akiteru Takamori [1], Kouseki Miyo [2]

[1] Earthquake Research Institute, the University of Tokyo

[2] Institute for Cosmic Ray Research, the University of Tokyo

1. Seismic/geodetic observation using laser strainmeters
2. Long-baseline laser strainmeter (GIF) in KAGRA
3. Low-frequency strain variations observed by GIF
4. Demonstration of the arm-length control of KAGRA



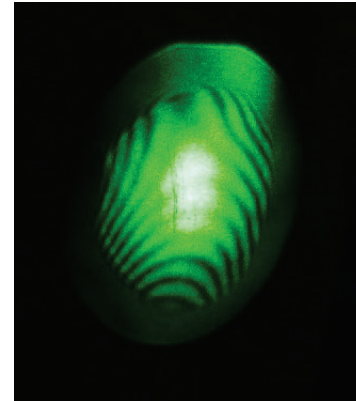
Low-frequency ground deformation observed by the geophysics interferometer (GIF) in the KAGRA tunnel

Akito Araya [1], Akiteru Takamori [1], Kouseki Miyo [2]

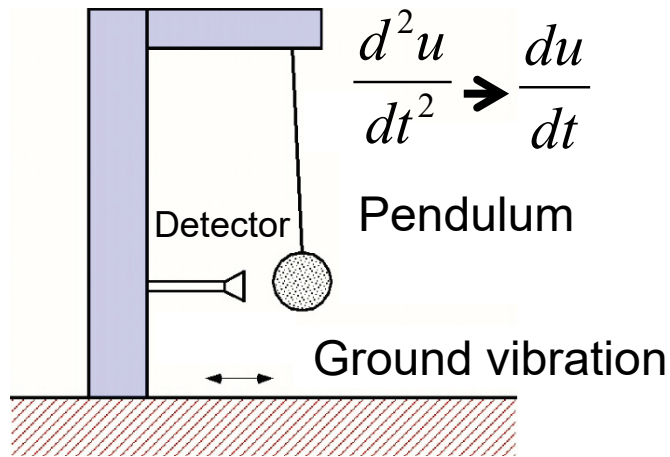
[1] Earthquake Research Institute, the University of Tokyo

[2] Institute for Cosmic Ray Research, the University of Tokyo

1. Seismic/geodetic observation using laser strainmeters
2. Long-baseline laser strainmeter (GIF) in KAGRA
3. Low-frequency strain variations observed by GIF
4. Demonstration of the arm-length control of KAGRA



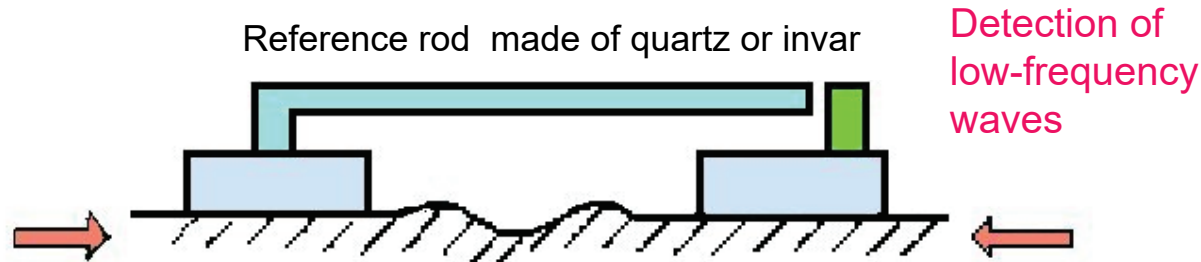
Seismometer and Strainmeter



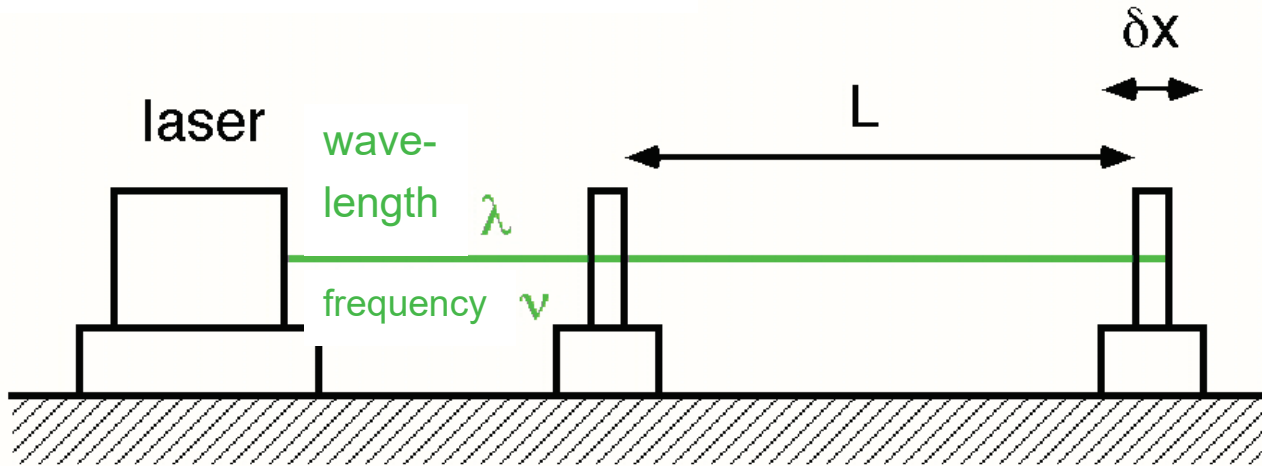
Seismometer
 --- Inertial sensor with cut-off f_c

$$\frac{u(x + dx) - u(x)}{L} \cong \frac{\partial u}{\partial x}$$

Strainmeter
 --- Measuring distance



Laser strainmeter (Vali et al., 1965)



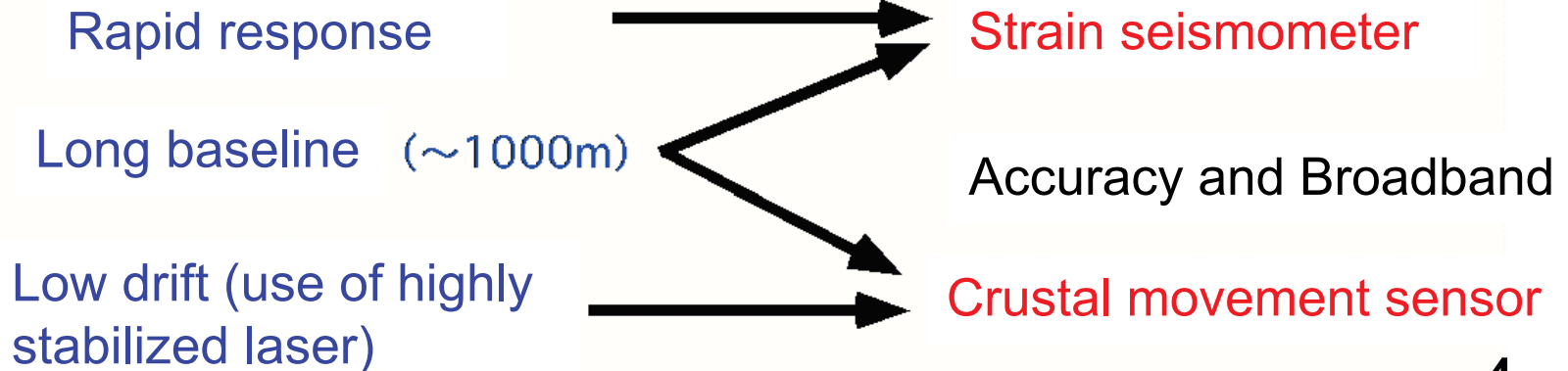
optical phase : $\phi = 2k(L + \delta x)$
($k = 2\pi/\lambda$)

strain : $\epsilon = \delta x/L = \underline{\delta \nu/\nu}$

Laser frequency stability

$\sim 10^{-13}$

Advantages of laser strainmeters ----- very broadband observation



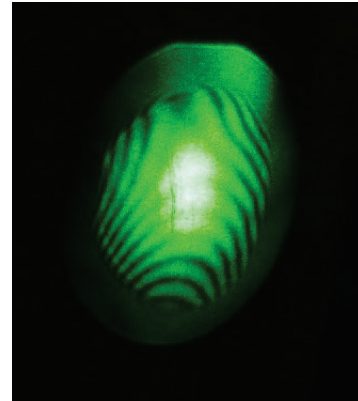
Low-frequency ground deformation observed by the geophysics interferometer (GIF) in the KAGRA tunnel

Akito Araya [1], Akiteru Takamori [1], Kouseki Miyo [2]

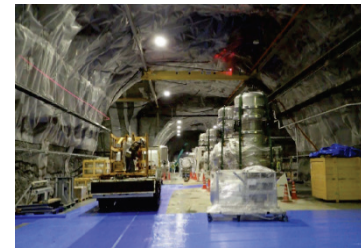
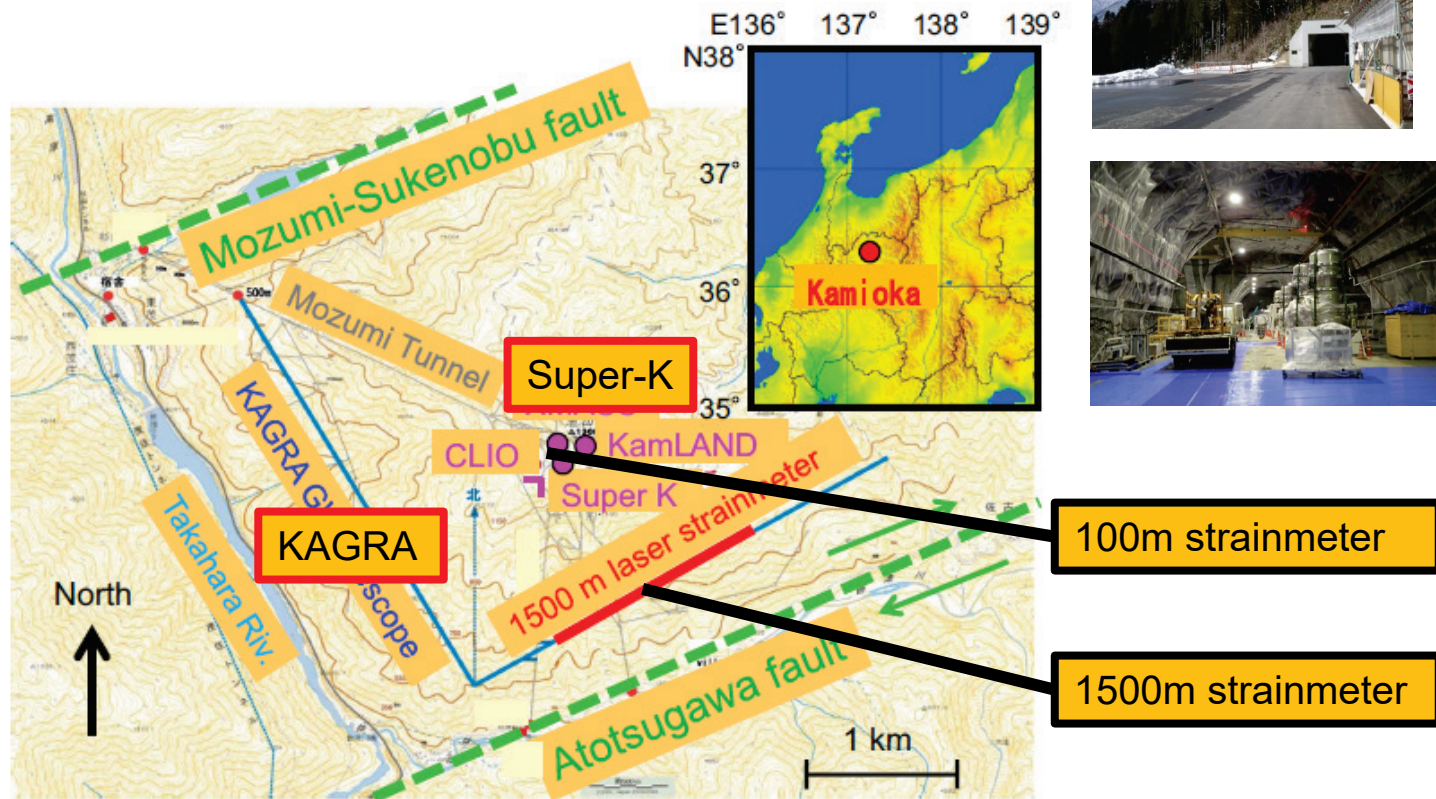
[1] Earthquake Research Institute, the University of Tokyo

[2] Institute for Cosmic Ray Research, the University of Tokyo

1. Seismic/geodetic observation using laser strainmeters
2. Long-baseline laser strainmeter (GIF) in KAGRA
3. Low-frequency strain variations observed by GIF
4. Demonstration of the arm-length control of KAGRA



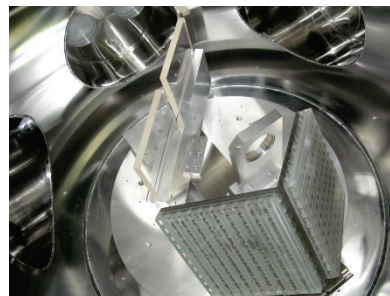
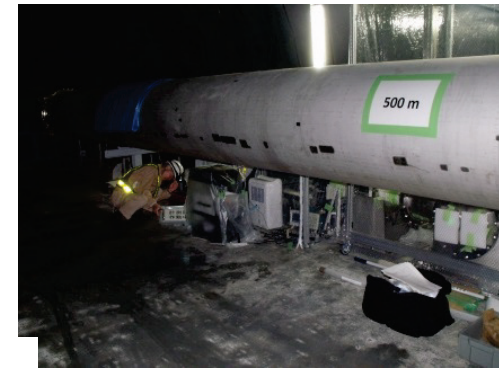
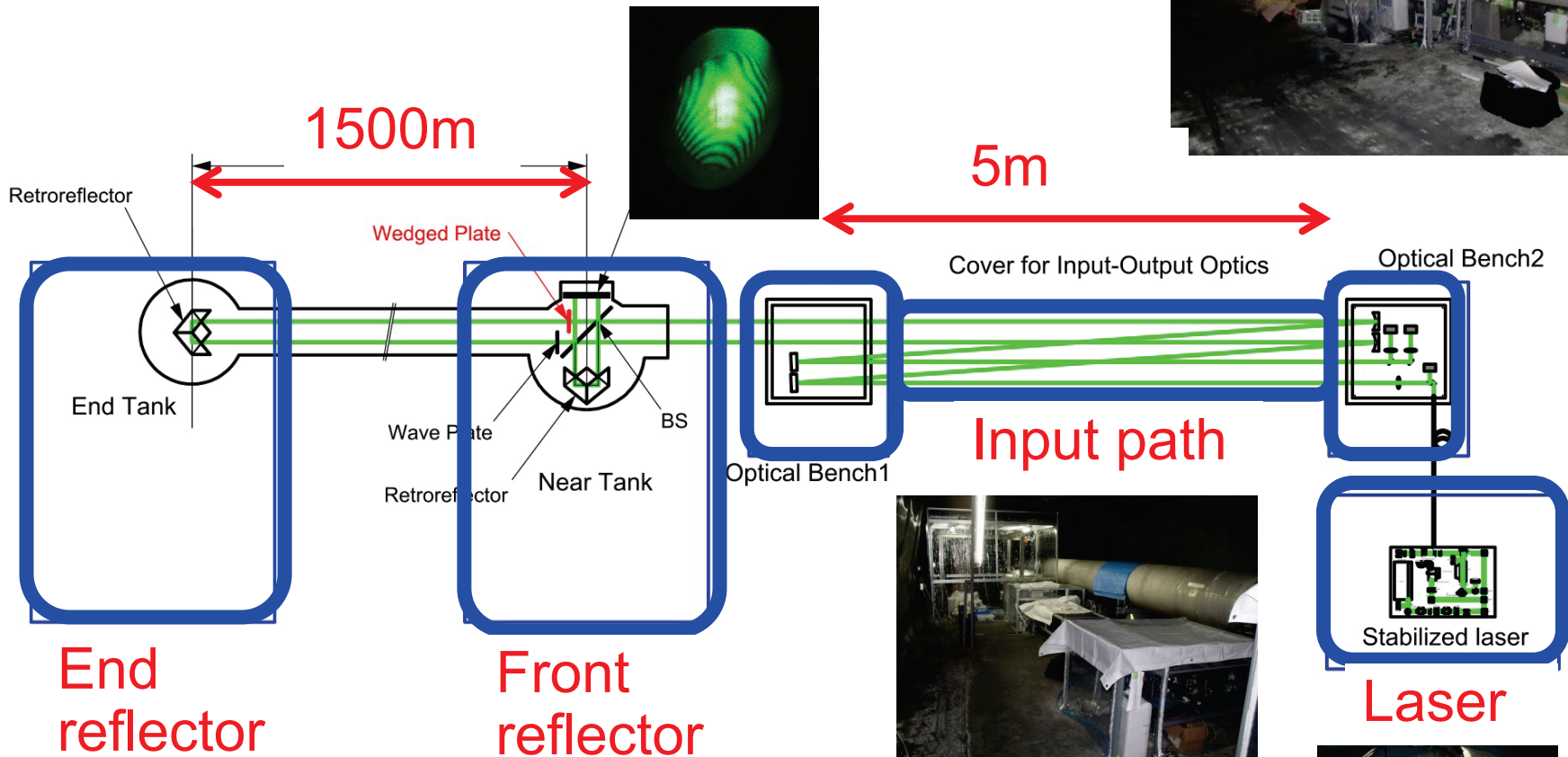
KAGRA baselines and fault locations (Cosmic Ray Research Institute, Univ. of Tokyo)



100m strainmeter

1500m strainmeter

Optical configuration of GIF-X

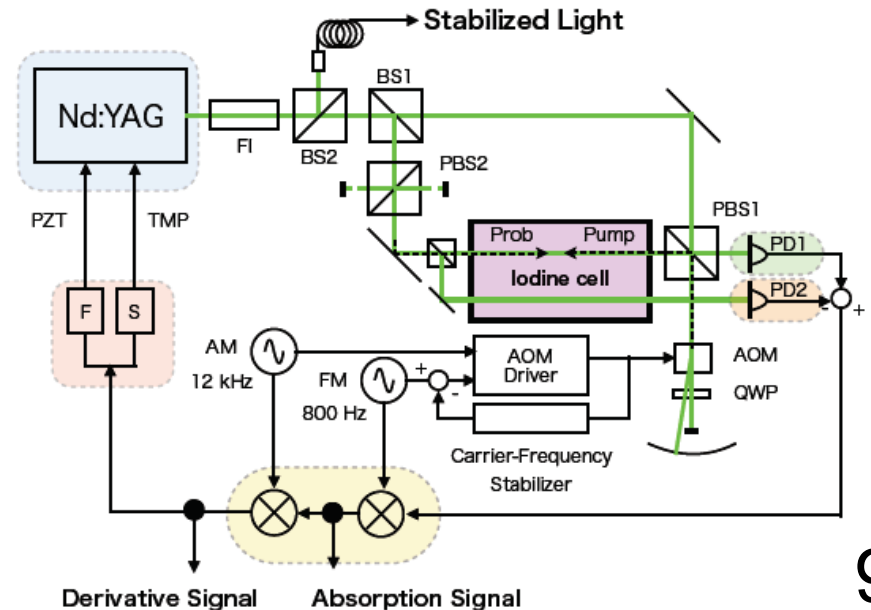
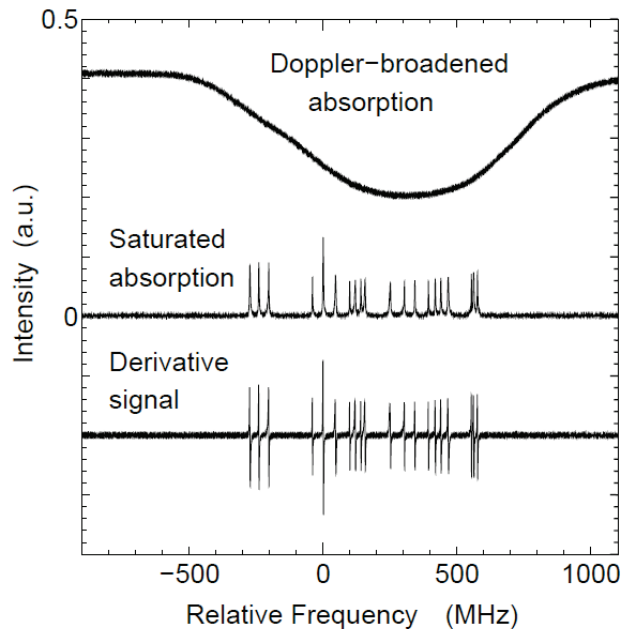
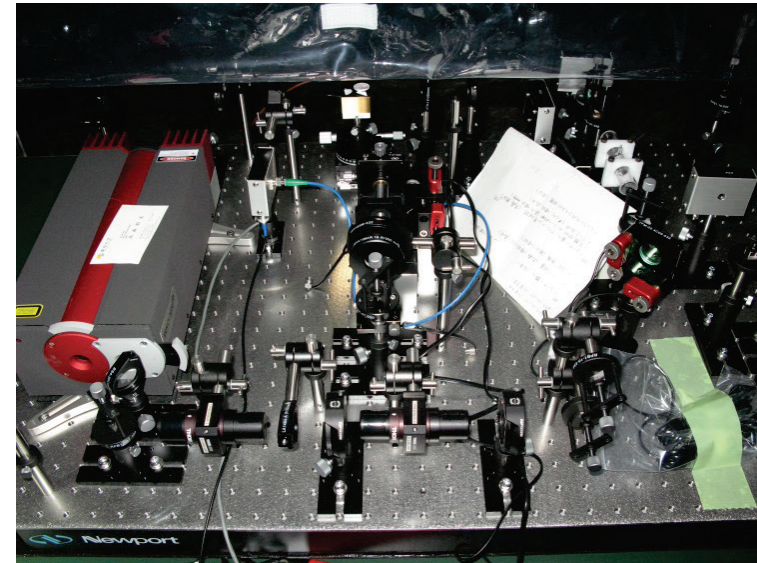


I₂ stabilized laser

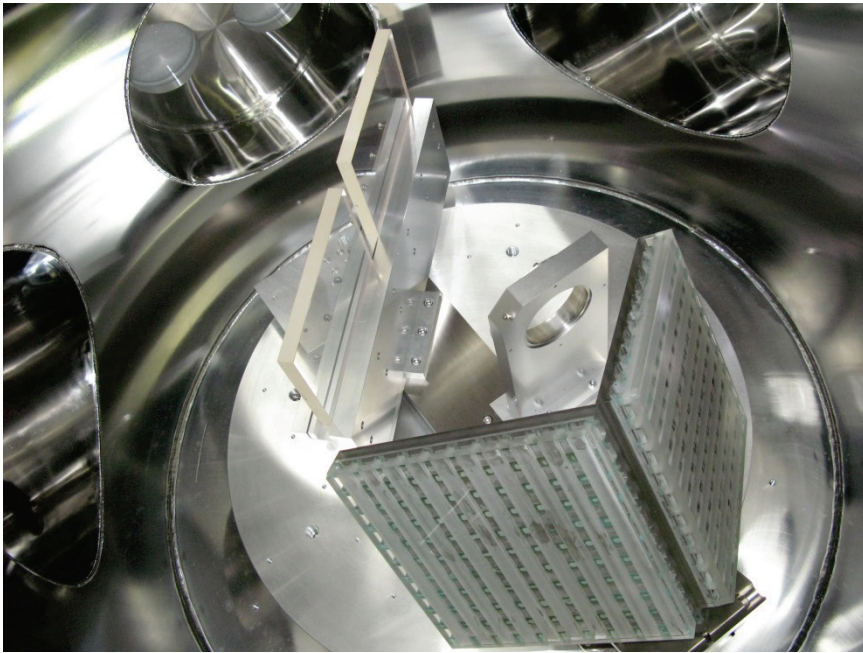
Locked to iodine Doppler-free absorption (532nm)

Stability of $\sim 10^{-13}$

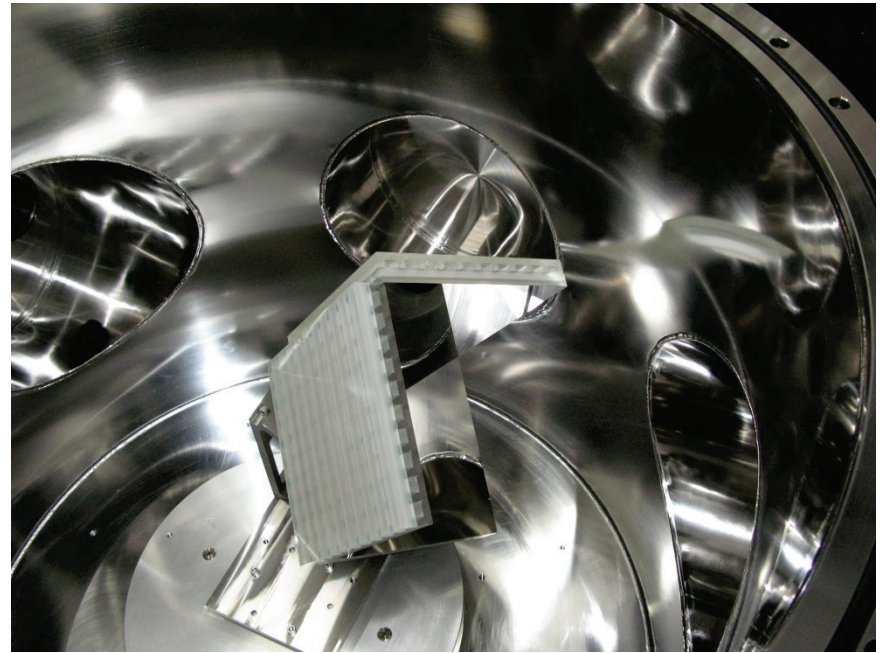
in Allan variance estimation



Beam splitters and retroreflectors (nominal aperture diameter: 15inch=38cm)

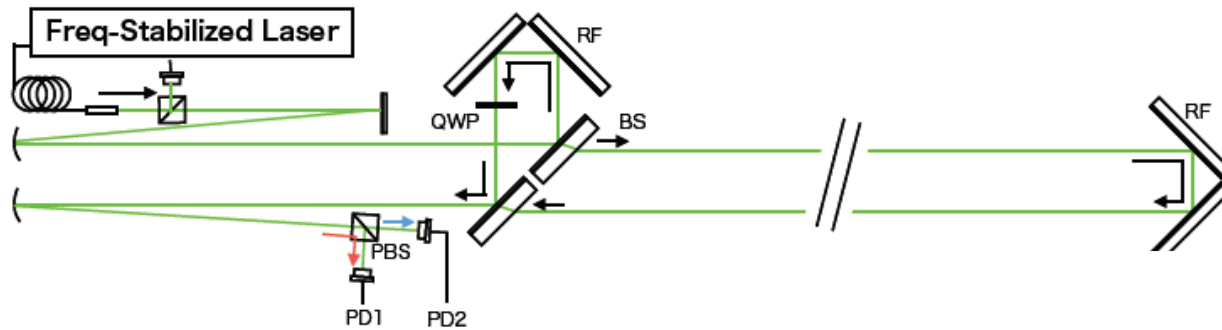
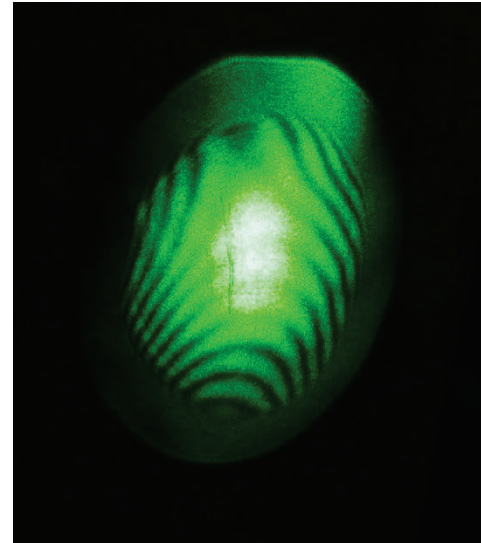
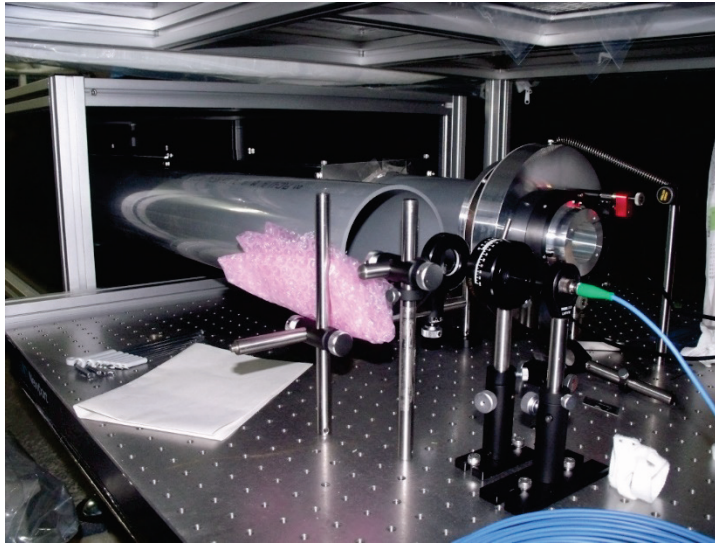


Optics in front tank

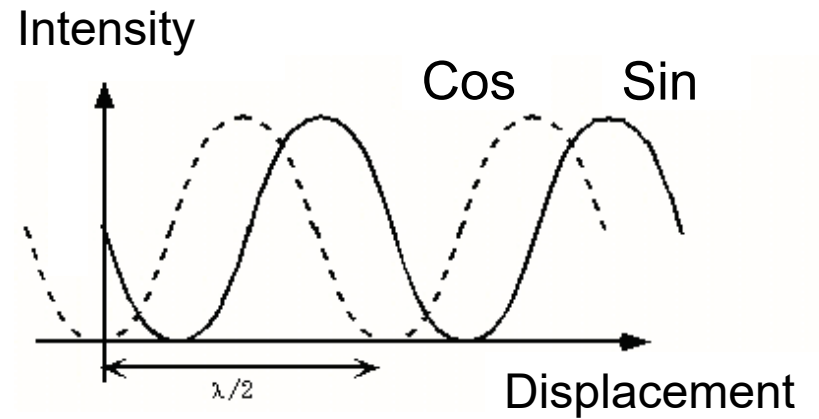
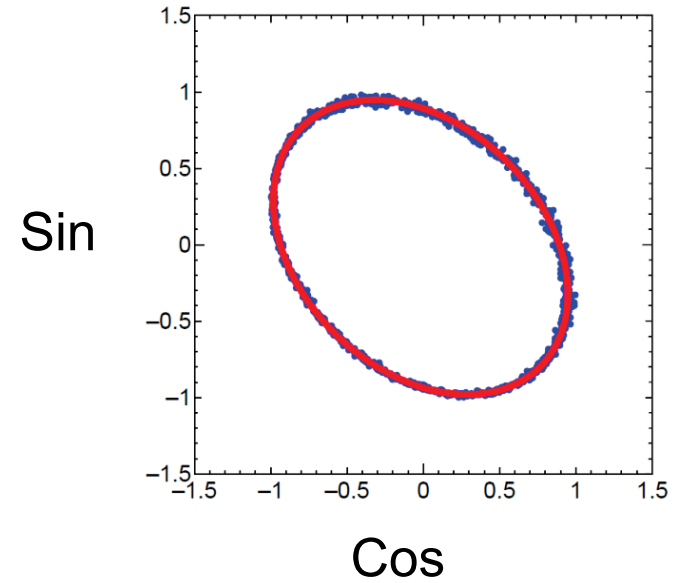
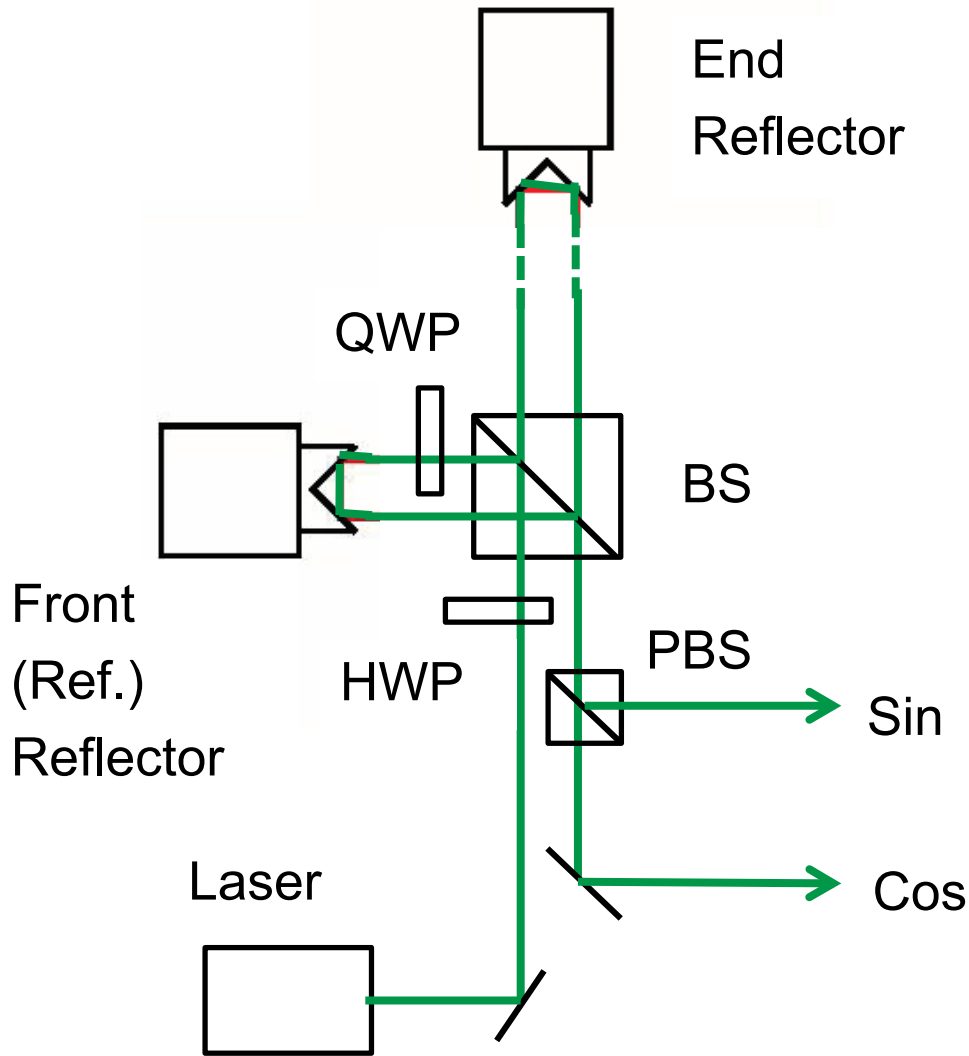


Retroreflector in end tank

Input optics (left) and interferometer fringe (right).



Quadrature Interferometer (no feedback to mirrors)



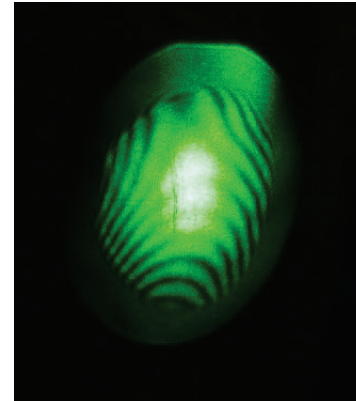
Low-frequency ground deformation observed by the geophysics interferometer (GIF) in the KAGRA tunnel

Akito Araya [1], Akiteru Takamori [1], Kouseki Miyo [2]

[1] Earthquake Research Institute, the University of Tokyo

[2] Institute for Cosmic Ray Research, the University of Tokyo

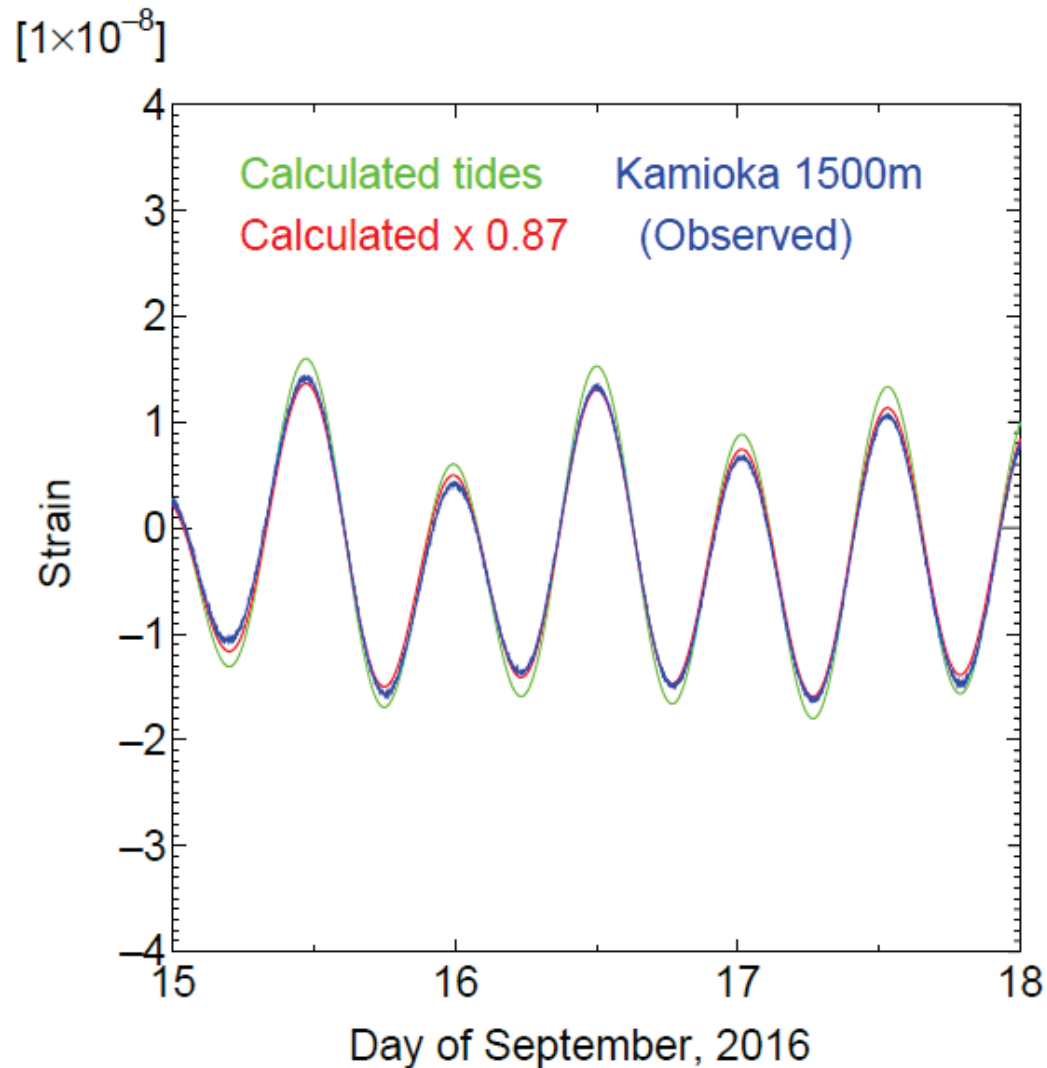
1. Seismic/geodetic observation using laser strainmeters
2. Long-baseline laser strainmeter (GIF) in KAGRA
3. Low-frequency strain variations observed by GIF
4. Demonstration of the arm-length control of KAGRA



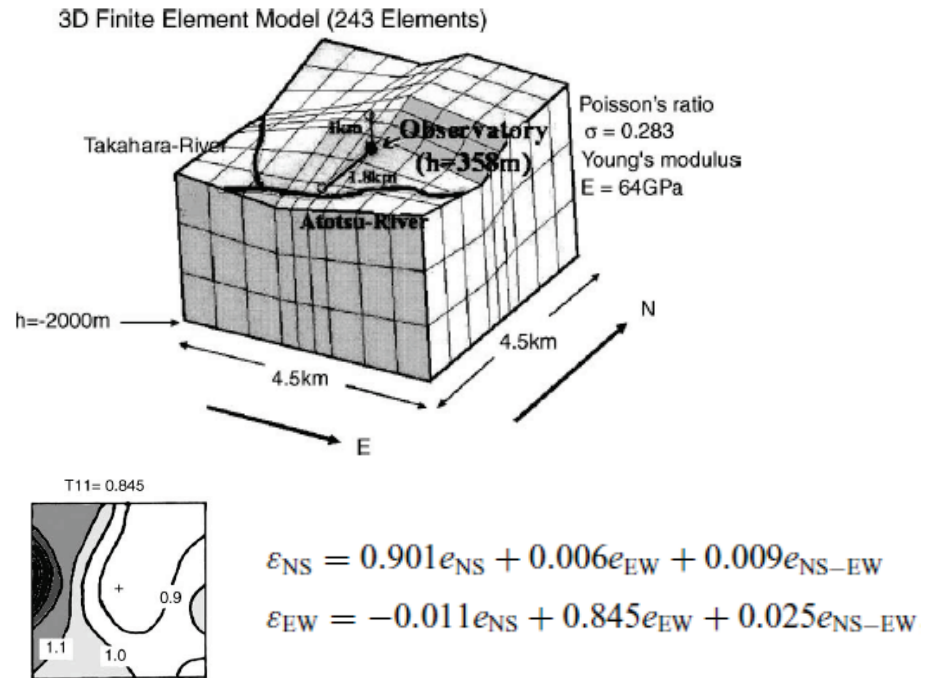
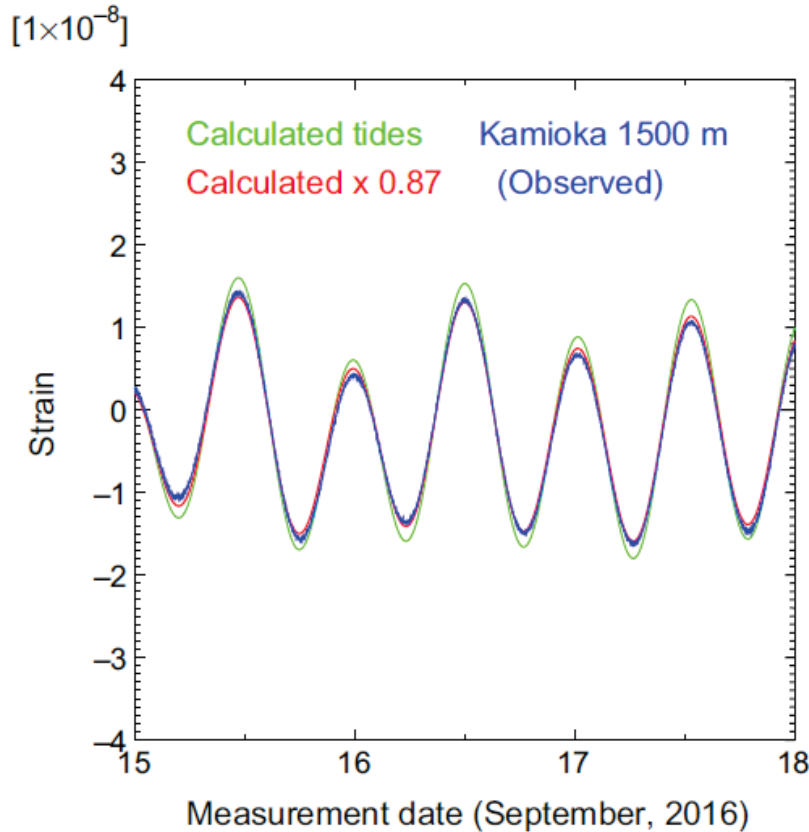
Earth tides --- $\sim 3 \times 10^{-8}$ in strain

Observed amplitude --- 0.87 of theoretical calc.

Earth tides are reduced by topographic effect



Observed Earth tides (left) and Topographic effects of underground site



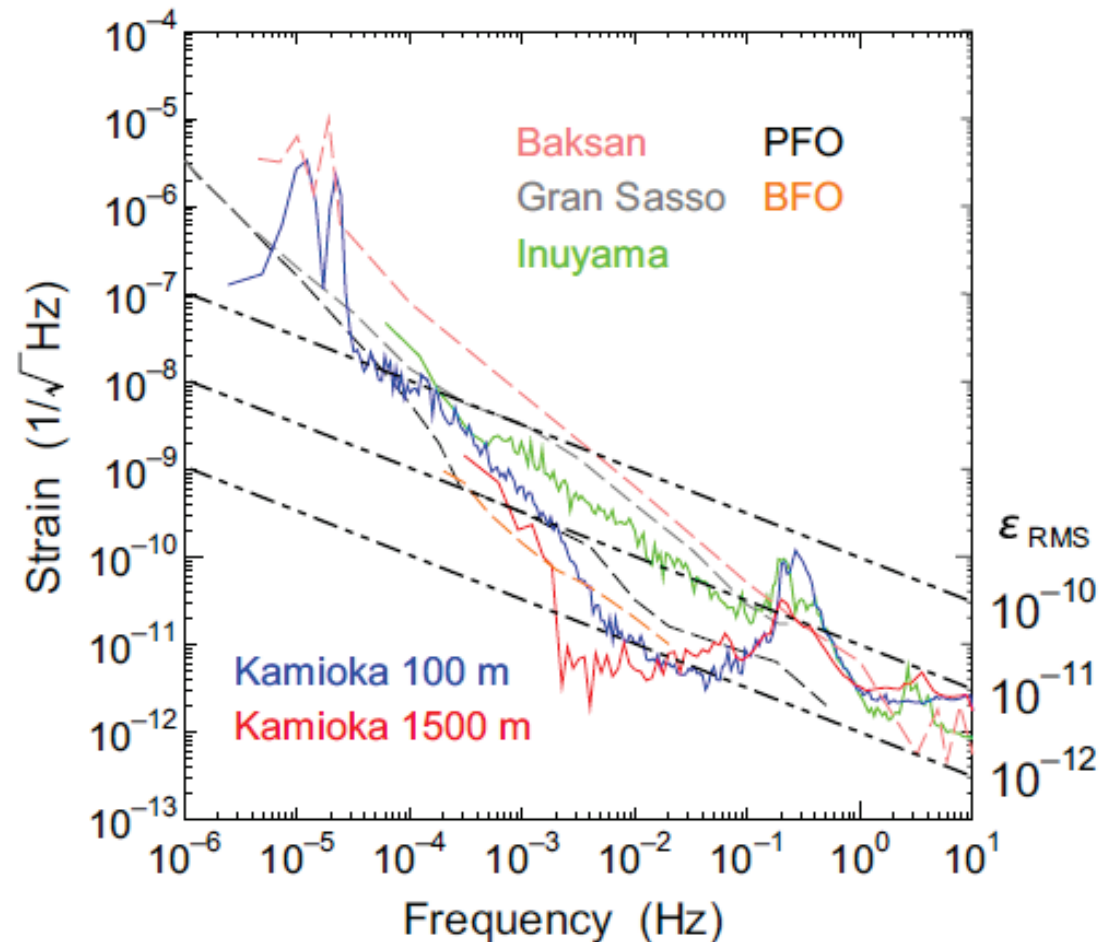
Reduction of tidal amplitude due to topography, 80-90% (Takemoto, 2006)

Strain spectra

Lowest background,
especially at around
(1-10) mHz

Capable of detecting
pico-strain level.

Araya et al., EPS, 2017.

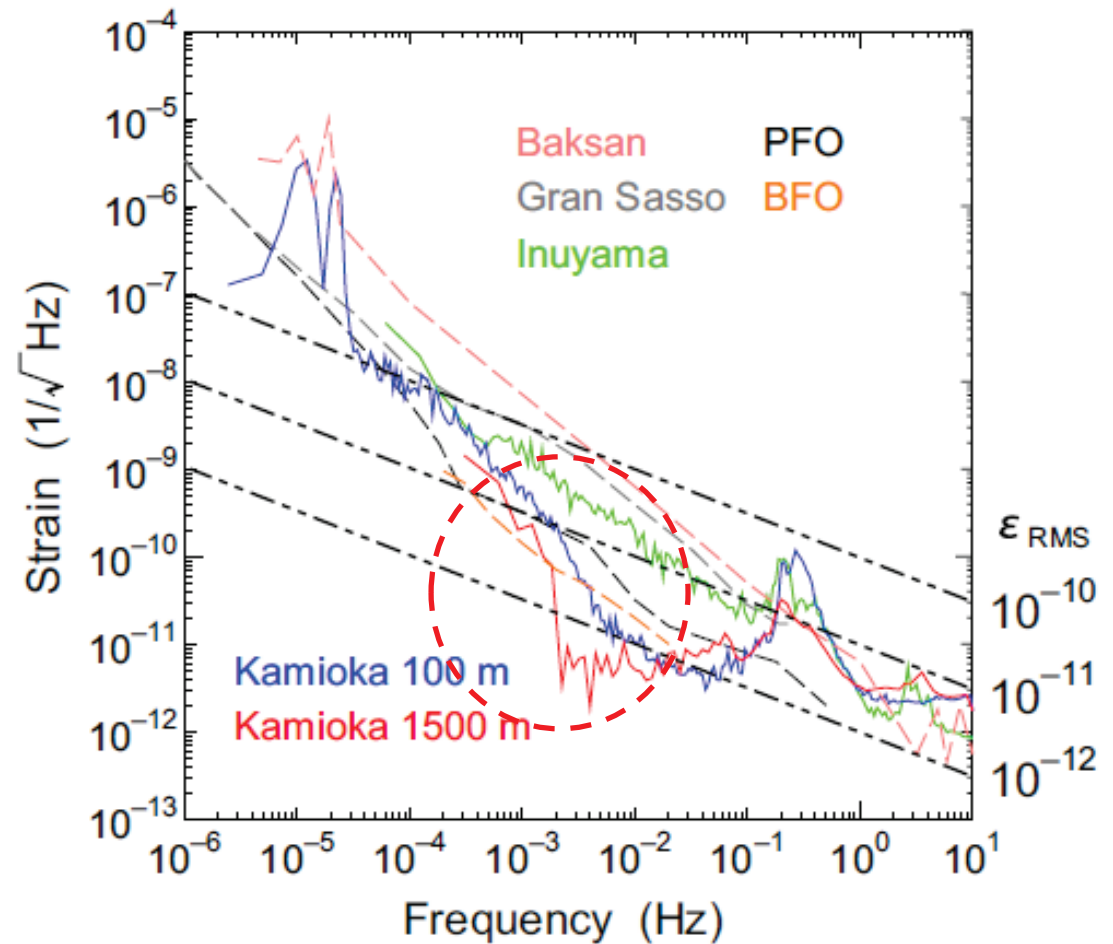


Strain spectra

Lowest background,
especially at around
(1-10) mHz

Capable of detecting
pico-strain level.

Araya et al., EPS, 2017.



Barometric response

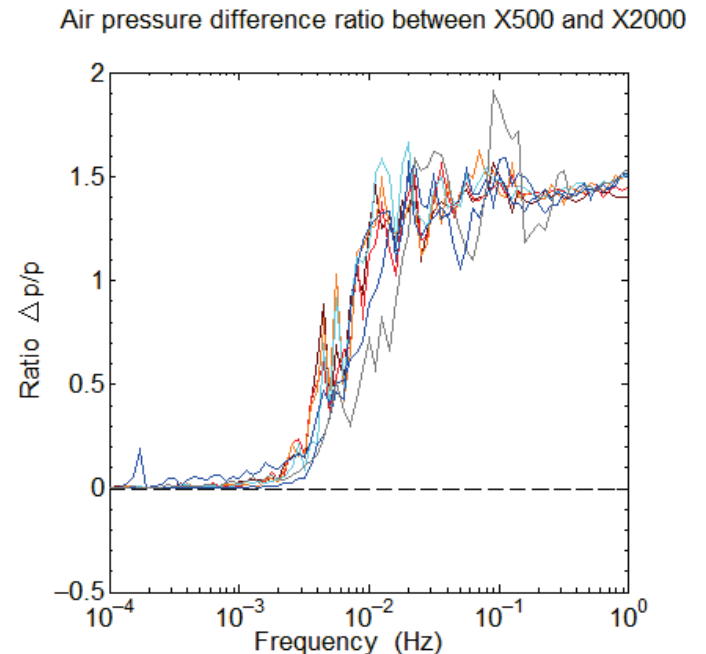
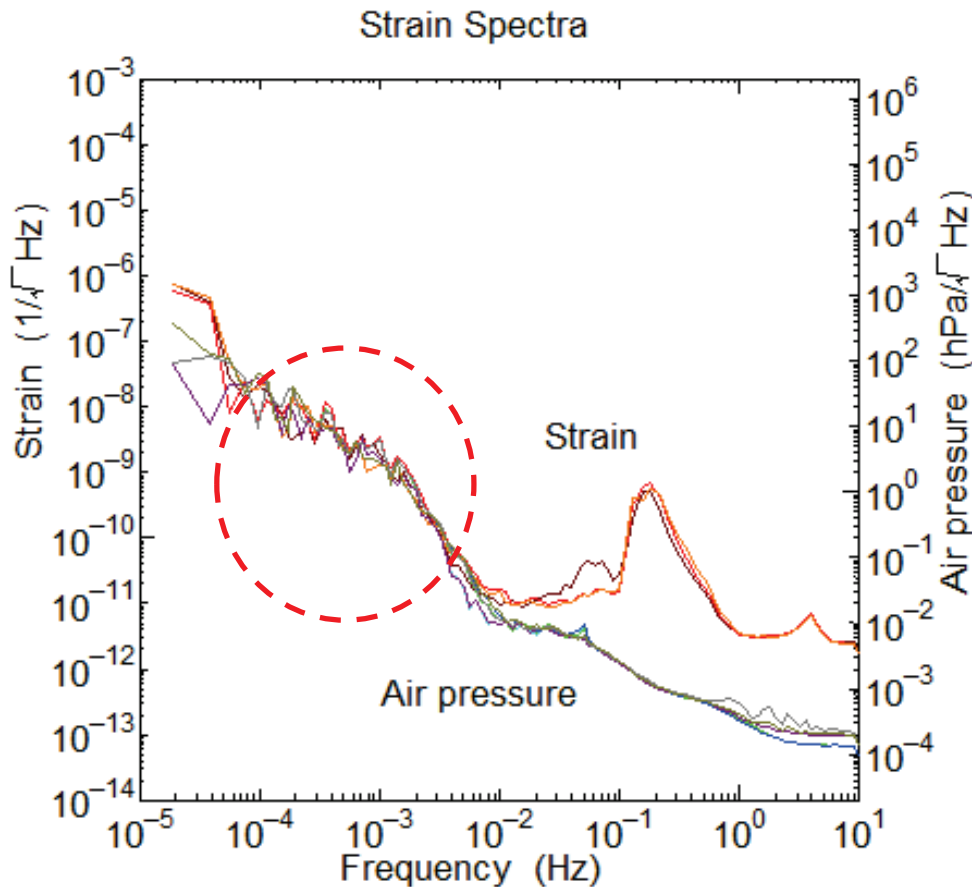
Strain in $10^{-4} - 10^{-3}$ -Hz region is highly dependent on the air pressure.

Barometric admittance

$\sim 0.55 \times 10^{-9} / \text{hPa}$

cf. $0.49 \times 10^{-9} / \text{hPa}$ (Zürn, 2015)

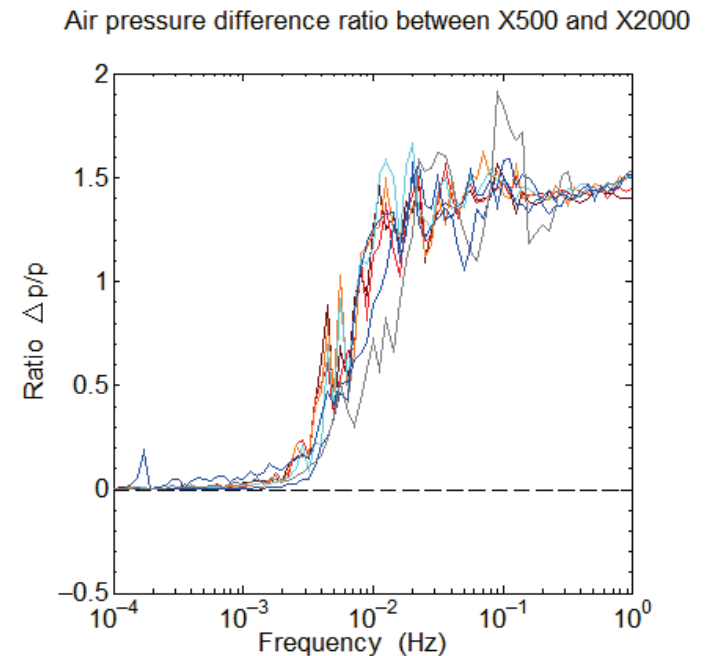
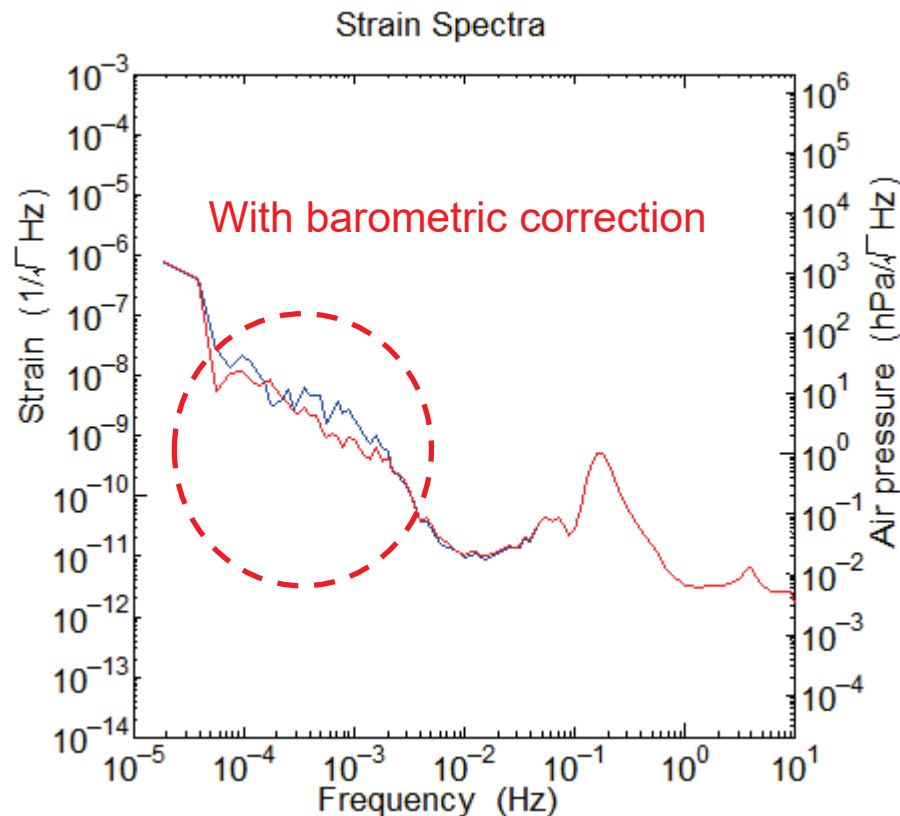
Air-pressure relative difference between X500 and X2000. Both air pressure are **identical (<10% difference)** below $\sim 3\text{mHz}$ and are **uncorrelated** above $\sim 10\text{mHz}$



Barometric response

- Barometric correction reduces strain background to $\sim 1/3$ in the $10^{-4} - 10^{-3}$ -Hz region.
- The limited reduction suggests response of ground to regional air pressure (**not the response of instruments** to the local air pressure).

T. Akutsu et al., PTEP, 2021



Long-term strains (June.- Sep. 2017)

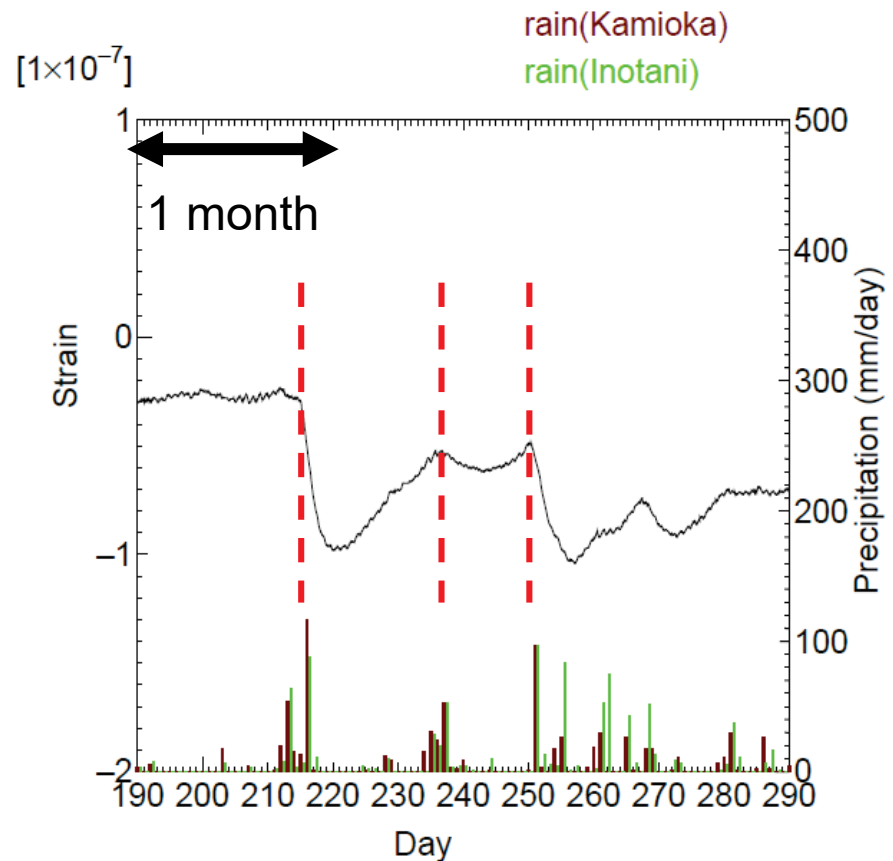
-Averaged for every 10 min.

-Theoretical tides were calculated and removed

Response to rain fall

.... due to change in load of groundwater ?

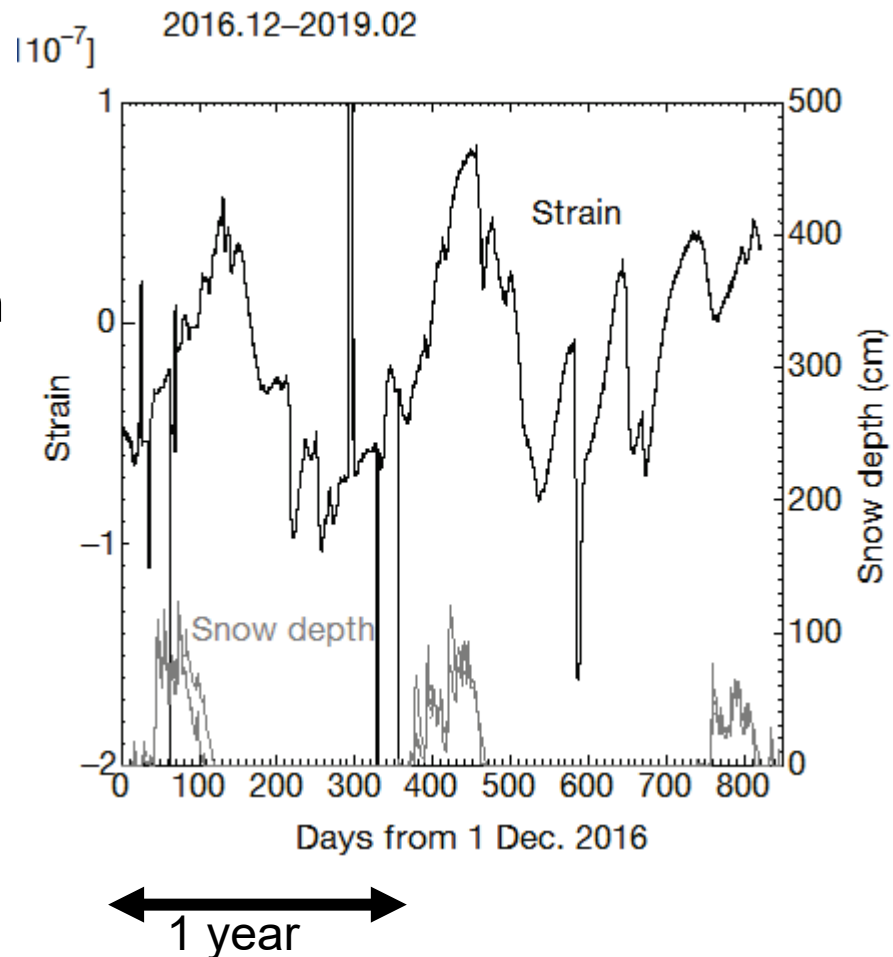
$\sim 5 \times 10^{-8}$ for 100mm rain-fall



Long-term strains (Dec. 2016 – Feb. 2019)

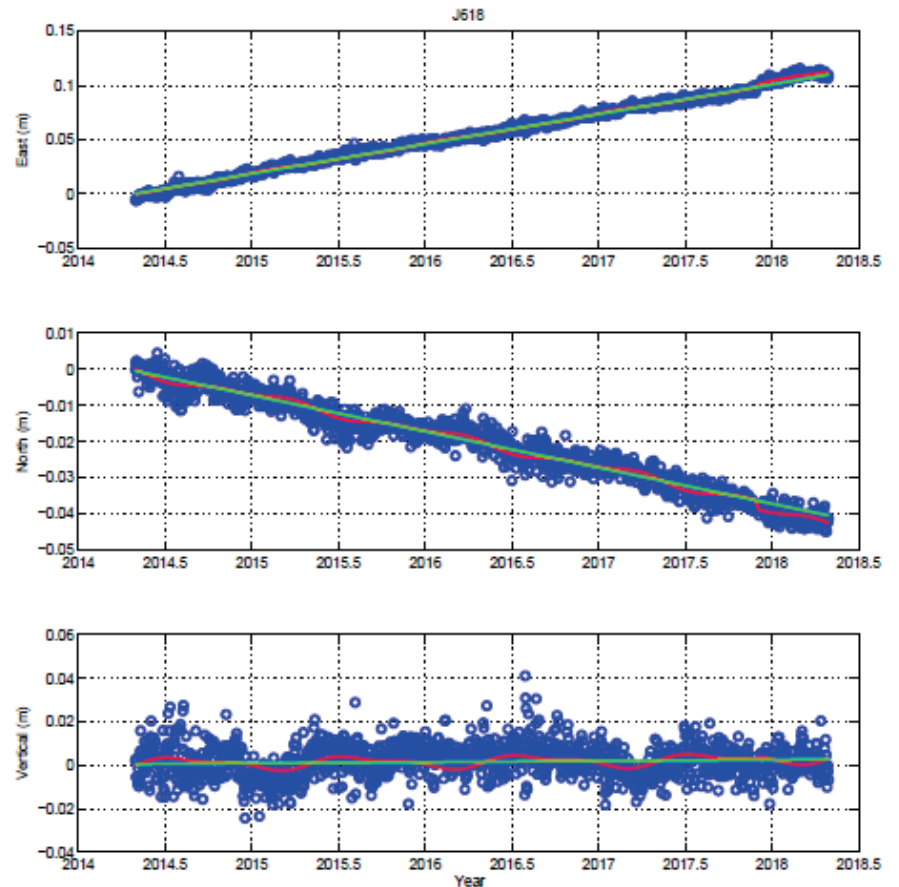
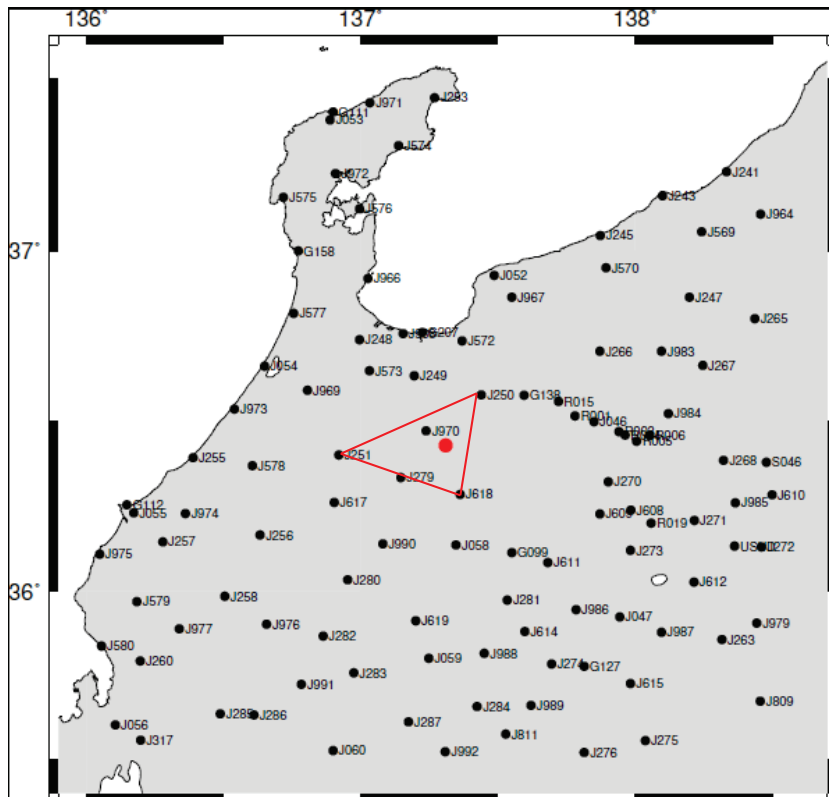
Response of snow load
 $\sim 3 \times 10^{-8}$ for 1-m snow depth

Data of snow depth (not at
the mountain) were
obtained from AMEDAS
(Inotani and Kamioka)



Long-term strains (Dec. 2016 – Feb. 2019)

Regional ground strain around KAGRA site measured by GNSS



Long-term strains (Dec. 2016 – Feb. 2019)

Rainfall response

$\sim 5 \times 10^{-8}$ /100-mm rainfall

Snow load response

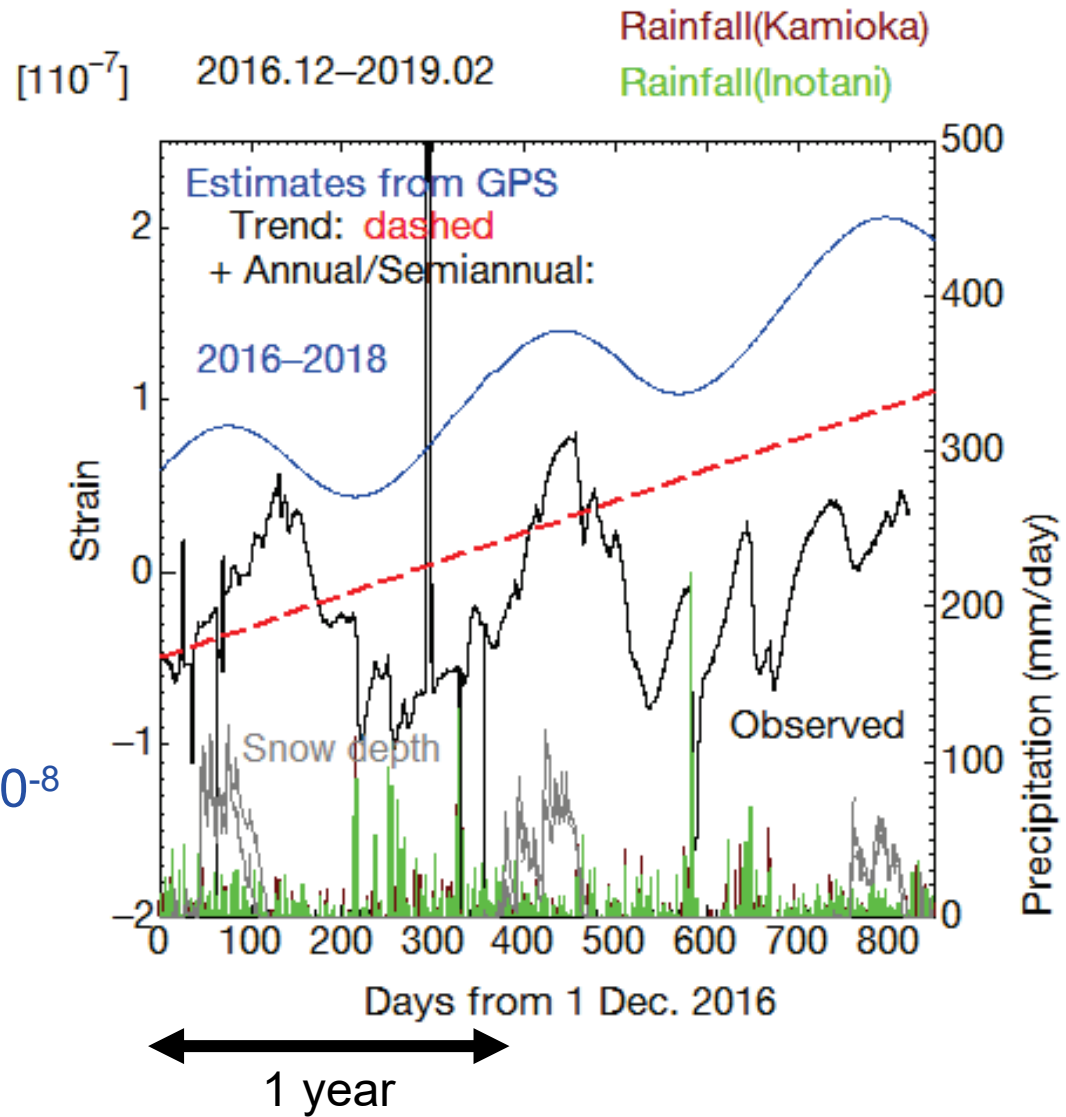
$\sim 3 \times 10^{-8}$ /1-m snow depth

roughly consistent

with GNSS estimates:

Trend: $\sim 7 \times 10^{-8}$ /year

Seasonal change: $\sim 6 \times 10^{-8}$



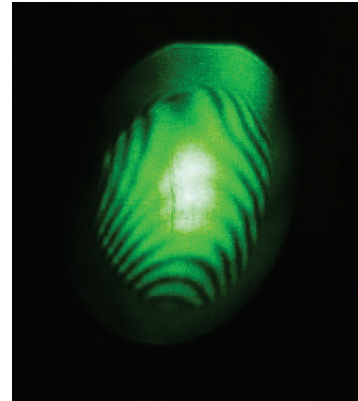
Low-frequency ground deformation observed by the geophysics interferometer (GIF) in the KAGRA tunnel

Akito Araya [1], Akiteru Takamori [1], Kouseki Miyo [2]

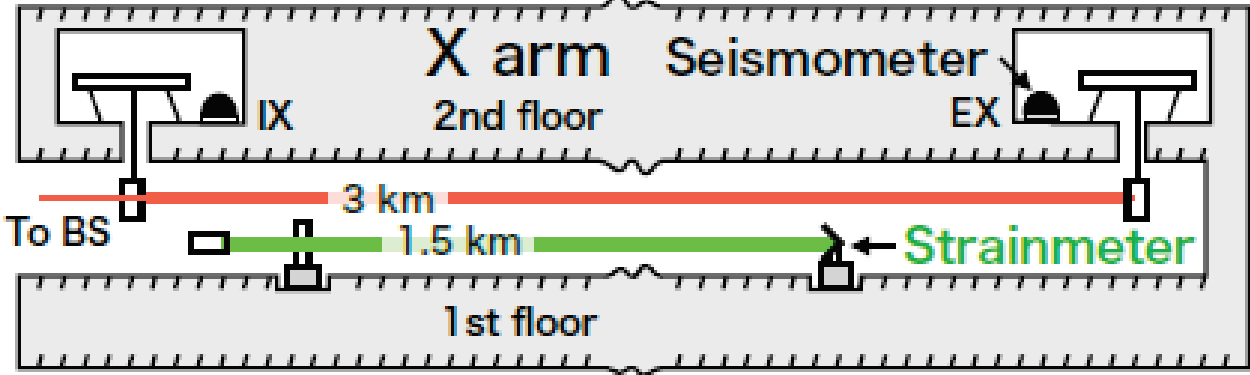
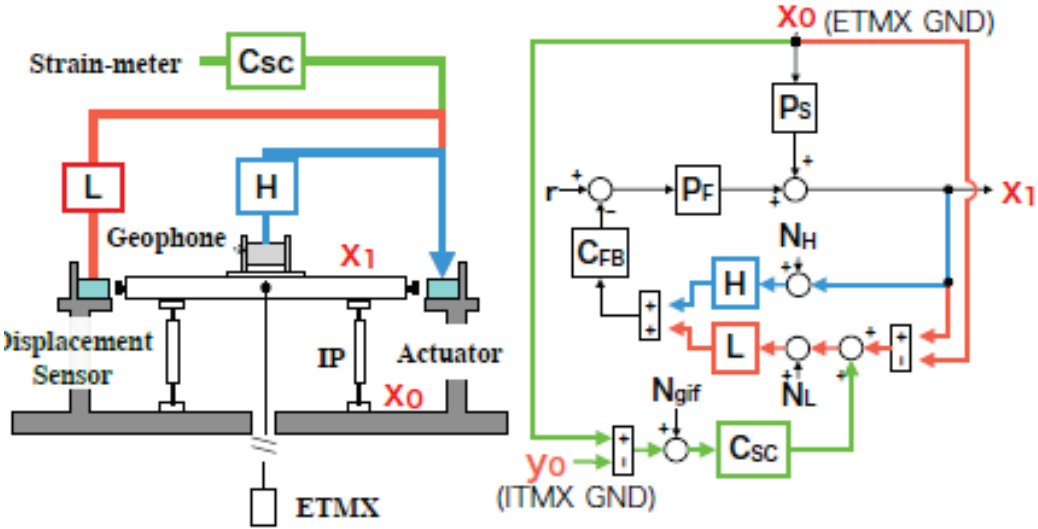
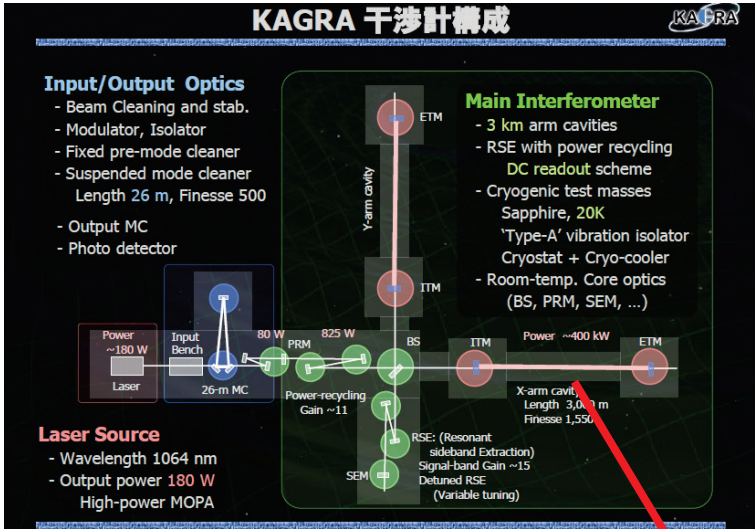
[1] Earthquake Research Institute, the University of Tokyo

[2] Institute for Cosmic Ray Research, the University of Tokyo

1. Seismic/geodetic observation using laser strainmeters
2. Long-baseline laser strainmeter (GIF) in KAGRA
3. Low-frequency strain variations observed by GIF
4. Demonstration of the arm-length control of KAGRA

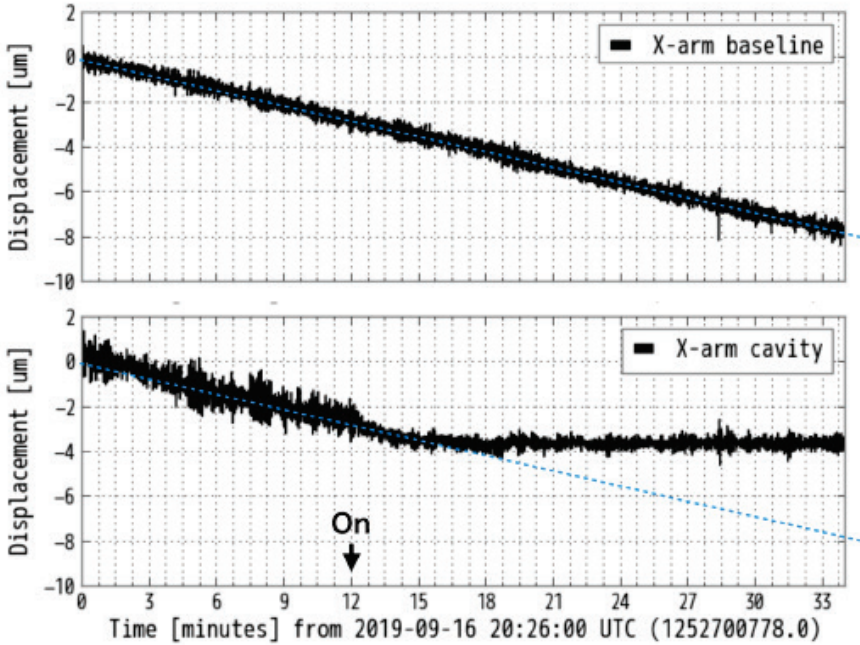
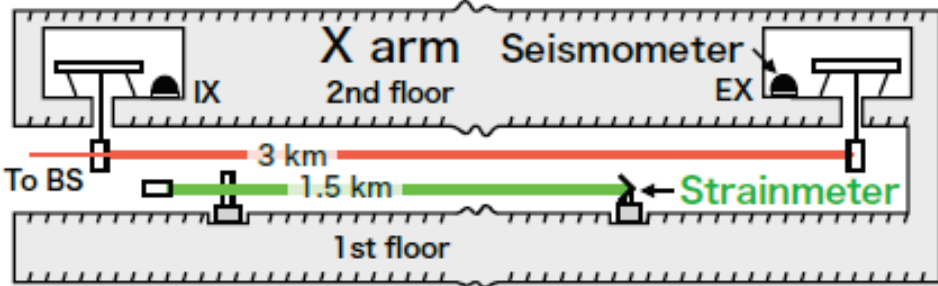


Feedforward control of arm length of KAGRA using the strainmeter signal.

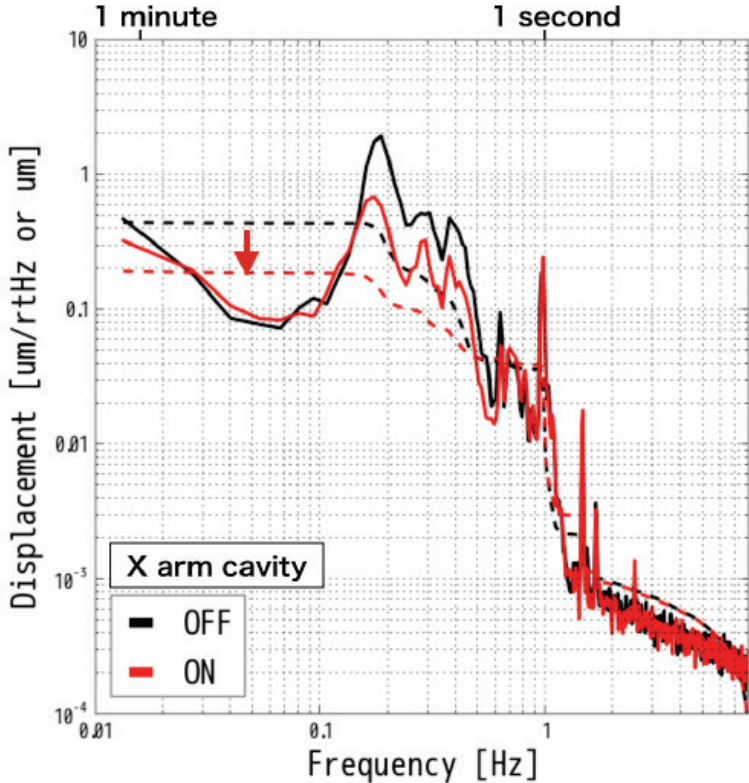


Feedforward control of arm length of KAGRA using the strainmeter signal.

T. Akutsu et al., PTEP, 2021



Baseline motions observed by the GIF (top) and the change in length of the KAGRA X-arm cavity (bottom).



RMS of cavity length mainly due to microseisms reduced to ~50 %

Conclusions

1. A 1500-m laser strainmeter in KAGRA has been in operation since 2016 and observed various ground strains at low frequencies.
2. Regional air pressures seem to affect ground strains in the millihertz band.
3. Temporal responses of ground strain to rainfall (contraction) and snow load (extension) was observed in Kamioka. Tectonic trends and seasonal changes are roughly consistent with estimates from GNSS.
4. Feedforward control of arm length of KAGRA using the strainmeter signal shows reduction of arm length change due to tides and microseisms.

Acknowledgment We used GEONET data. The data were analyzed by Dr. J. Fukuda (ERI). This research was supported in part by Kakenhi.